HAL
open science

Photoisomerization of IC3N - An experimental and theoretical study

A. Guzik, M. Gronowski, M. Turowski, Jean-Claude Guillemin, R. Kolos

To cite this version:

A. Guzik, M. Gronowski, M. Turowski, Jean-Claude Guillemin, R. Kolos. Photoisomerization of IC3N - An experimental and theoretical study. Journal of Photochemistry and Photobiology A: Chemistry, 2020, 395, pp.112470. 10.1016/j.jphotochem.2020.112470 . hal-02569948

HAL Id: hal-02569948

https://univ-rennes.hal.science/hal-02569948v1

Submitted on 12 May 2020

HAL is a multi-disciplinary open access archive for the deposit and dissemination of scientific research documents, whether they are published or not. The documents may come from teaching and research institutions in France or abroad, or from public or private research centers.

L'archive ouverte pluridisciplinaire **HAL**, est destinée au dépôt et à la diffusion de documents scientifiques de niveau recherche, publiés ou non, émanant des établissements d'enseignement et de recherche français ou étrangers, des laboratoires publics ou privés.

Journal Pre-proof

Photoisomerization of IC_3N. An experimental and theoretical study.

A. Guzik,[a] M. Gronowski,[b] M. Turowski,*[,b,c] J.-C. Guillemin,[d] R. Kołos [b]

[a] Cardinal Wyszyński University, Faculty of Mathematics and Natural Sciences, School of Exact Sciences, Wóycickiego 1/3 building 21, 01-938 Warsaw, Poland.

[b] Institute of Physical Chemistry, Polish Academy of Sciences, Kasprzaka, 44/52, 01-224 Warsaw, Poland.

[c] Department of Chemistry and Biochemistry, University of Colorado, Boulder, Colorado 80309-0215, United States.

[d] Univ Rennes, Ecole Nationale Supérieure de Chimie de Rennes, CNRS, ISCR – UMR6226, F-35000 Rennes, France.

* corresponding author, mturowski@protonmail.com

Graphical Abstract

Journal Pre-proof

Journal Pre-proof

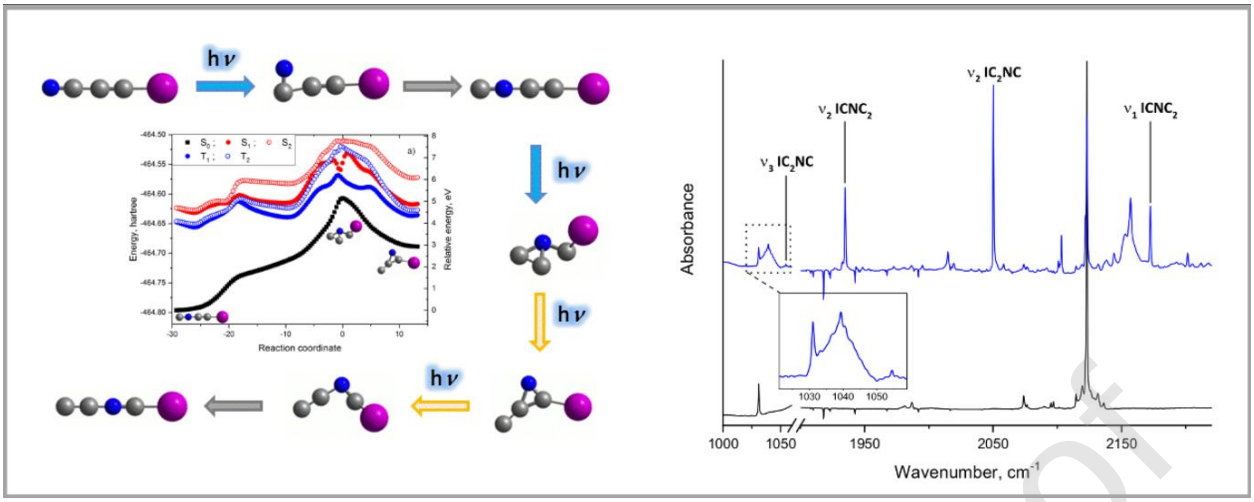

Highlights

- VUV photolysis of IC_3N in argon matrix leads to IC_2NC and $ICNC_2$ isomers
- IRC calculations show reaction paths leading to discovered isomers
- IC_3N ions and radical are not formed in detectable amounts for the IR absorption

ABSTRACT: Here we present the results of a joint spectroscopic and quantum chemical study on the photochemistry of 3-iodo-2-propynenitrile (iodocyanoacetylene, IC_3N). Vacuum-UV photolysis of the compound isolated in solid argon was explored. Calculations, carried out at the DFT and/or coupled-cluster level of theory, provided essential data concerning the thermodynamic stabilities, vibrational and electronic energy levels, ionization potentials, and electron affinities of IC_3N-stoichiometry isomers and ions. The photochemical formation of thus far unknown species IC_2NC and $ICNC_2$ has been evidenced by the experiment and rationalized based on a detailed theoretical approach, involving the excited-state potential energy surfaces.

KEYWORDS: photochemistry, cyanoacetylenes, matrix isolation, IR spectroscopy, computational chemistry

1. Introduction

The direct motivation for this study stems from a larger project devoted to the photochemistry of small alkynylcarbonitriles. In particular, former investigations on

Journal Pre-proof

cryogenically isolated, UV-irradiated HC_3N and HC_5N have shown the wealth of photoproduced isomers, some of which being highly energetic and feature unusual chemical bonding.[1–3] Isomerization could be anticipated also for IC_3N. Moreover, it was of interest to check whether photolyzed IC_3N could be an efficient source of C_3N^-, opening the way towards better characterization of this anion (HC_3N and HC_5N photolyses yielded C_3N^- and C_5N^-, respectively, but in small amounts).

Kloster-Jensen et al. published on the location of IR and UV absorption bands of IC_3N, [4] as well as on the electric dipole moment (4.59 D) of this nitrile, inferred from microwave spectra. Its Raman spectroscopy has also been studied.[5,6] Linearity of the molecule was confirmed with X-ray diffraction measurements.[7] Bieri et al. and Kuhn et al. measured the photoelectron spectra.[8,9] To our knowledge, no photochemical studies of IC_3N have ever been reported.

2. Experimental and computational methods

IC_3N was synthesized on a preparative scale by the method of Kloster-Jensen, involving the reaction of HC_3N with I_2/KI alkaline solution.[4] The product was characterized by ^{13}C NMR spectroscopy: ^{13}C NMR ($(CD_3)_2CO$, 100 MHz) δ 22.4 (s, C-I), 67.8 (s, C-CN); 106.1 (s, CN). The chemical shift of the sp carbon next to the iodine atom, observed at high-field, is characteristic of iodoalkynes. Traces of HC_3N could not be completely removed by freeze-pump-thaw cycles.

Gaseous IC_3N was mixed with Ar (Multax s.c.) in ratios ranging from 1:600 to 1:1100, in a vacuum manifold equipped with capacitance manometers (MKS Instruments). Mixtures were deposited at a rate of about 2 mmol/h onto a CsI substrate window, the latter attached to the cold finger of an Air Products *Displex* DE-202S cryostat. In photochemical experiments, the window was continuously VUV-irradiated (see below) throughout the sample deposition. The window was held either at 15-17 K or, exclusively during VUV irradiations, at 19 K. For electronic spectroscopy measurements, gaseous IC_3N (0.13 Torr at room temperature) was mixed with 100 Torr of argon in a 10-cm glass cuvette equipped with quartz windows. Spectra were recorded in the 205-700 nm range with a resolution of 1.0 nm, using a Shimadzu UV-3100 instrument. A Nicolet *Magna* 560 FTIR spectrometer was used for IR absorption measurements in the 4000 - 400 cm^{-1} range with a resolution of 0.5 cm^{-1}.

Journal Pre-proof

For far-UV photolysis experiments, a microwave-driven Kr discharge lamp (Opthos Instrument Comp.) was attached to the vacuum shroud of the cryostat, about 5 cm from the sample substrate. The lamp, operated at 20 W, had a broadband spectral characteristic (127-160 nm) with a maximum near 145 nm; the emitted beam was not focused. The slightly elevated deposition temperature (19 K) was applied to boost the photochemical processes.

The Becke's three-parameter hybrid exchange functional including the correlation functional of Lee, Yang, and Parr (B3LYP) was selected for the majority of DFT calculations.[10] [11] The Dunning's correlation-consistent polarized valence triple-zeta basis set,[12] augmented by s, p, d, and f functions (aug-cc-pVTZ) was used for N and C, while for the I atom a basis set with pseudopotentials (hereafter: PP) was employed.[13] Geometric structures, energies, and harmonic frequencies were calculated for IC_3N, its isomers, and several other potential photolysis products. The harmonic frequencies were scaled with a factor of 0.96 to correct for anharmonicity and for other inherent deficiencies of the DFT approach.[14,15] Transition states were localized on the electronic ground state potential energy surface (PES) using the Berny algorithm.[16] Their nature was verified by inspection of vibrational frequencies (exactly one imaginary frequency was expected). Further IRC (intrinsic reaction coordinate) calculations indicated the geometries of species linked by a given transition state.[17] In order to describe the mechanism of a photo-induced reaction, knowledge of excited PESs is crucial. Both triplet and singlet excited electronic state energies were calculated using the time-dependent DFT (TD-DFT) version.[18–20] The Tamm-Dancoff approximation was applied, as it was reported to perform well for numerically unstable cases and was found to provide reliable singlet-triplet separations.[21–25] Excited-state PES landscapes were approximated using vertical excitations for a series of geometries obtained with ground-state IRC calculations.

The geometries of selected lowest excited states of IC_3N and IC_2NC were optimized with the B3PW91 functional and the same basis sets as for the ground state. B3PW91 (differing from B3LYP by a PW91 non-local correlation term)[26–28] has already been successfully used to describe some excited electronic states of cyanoacetylene family molecules, including HC_9N,[29] CH_3-C_3N,[30] and CH_3-C_5N.[31] We verified the reliability of B3PW91-derived vertical excitation energies by applying also the CAM-B3LYP functional [32] with large basis sets (aug-cc-pVQZ for C and N, and aug-cc-pVQZ-PP for the I atom).[12,33]

Journal Pre-proof

Second order perturbation theory (VPT2) was used to predict anharmonic vibrational frequencies and intensities for fundamental,[34–36] overtone, and combination bands, at the B3LYP level of theory. All DFT calculations were carried out using the Gaussian 09 Rev. E. 01 set of programs.[37] The vibrational self-consistent field (VSCF)[38,39] and correlation-corrected vibrational self-consistent field (VMP2)[39,40] methods were also used to compute anharmonic fundamental frequencies using a frozen-core version of CCSD(T) (coupled-cluster singles and doubles with perturbative treatment of triples).[41–46] These two different approaches, VSCF and VMP2, were chosen to check for consistency of the resulting frequencies (variational VSCF computations are not as sensitive to resonance-related artifacts as those carried out with the perturbation methods VMP2 and VPT2. An efficient approach was used in VSCF and VMP2 calculations to generate potential energy surfaces around the equilibrium structures.[47–49] Fundamental harmonic frequencies were numerically derived, [50,51] for the previously optimized [52] structures. One- and two-body terms were included. For CCSD(T) computations, Dunning's correlation-consistent polarized valence triple-zeta basis set (cc-pVTZ)[12] was selected for N and C, while a basis set with pseudopotentials (cc-pVTZ-PP)[13] was used for the I atom. All ab initio calculations of anharmonic vibrational frequencies were performed with the Molpro 2012.1 software.[53,54] Computational results were visualized using ChemCraft.[55]

3. Results and discussion

Electronic spectroscopy

Table 1 contains vertical electronic excitation energies and the respective oscillator strengths computed by CAM-B3LYP/aug-cc-pVQZ for IC_3N. Optimization of excited-state structures starting from a linear geometry using B3PW91/aug-cc-pVTZ failed for most states or led to imaginary frequencies. This suggested a non-linearity of these states. Indeed, our search for the equilibrium geometry of the lowest excited singlet (S_1) and triplet (T_1) revealed the bent structures (Figs. S1 and S2). Similar computations were performed for IC_2NC, a likely photochemical product arising from UV irradiation of IC_3N (see Table S1 and Figs. S1-S2 of the Supplementary material). The predicted 0-0 (i.e. vibrationless) energies of S_1-S_0 excitations are 3.3 eV and 3.2 eV (TD-B3PW91/aug-cc-pVTZ) for IC_3N and IC_2NC, respectively.

Journal Pre-proof

A UV-Vis spectrum of gaseous IC_3N is presented in Fig. 1. The molecule is a strong absorber. One can discern a structure resembling that previously reported, namely the bands at 222, 233, 245 and 262 nm, measured by Kloster-Jensen et al. in a cyclohexane solution.[56] The band pattern is similar to the one known for HC_3N,[57–59] but IC_3N bands are distinctly broader.[30] The spectrum shows clear maxima at 44 400, 41 400, 39 300, and 36 600 and cm^{-1} (225, 242, 254, and 273). According to the predictions of Table 1, there are three closely spaced electronic states around 250 nm. While at least one of these is responsible for the said (presumably vibronic) bands, no reliable assignments can currently be proposed.

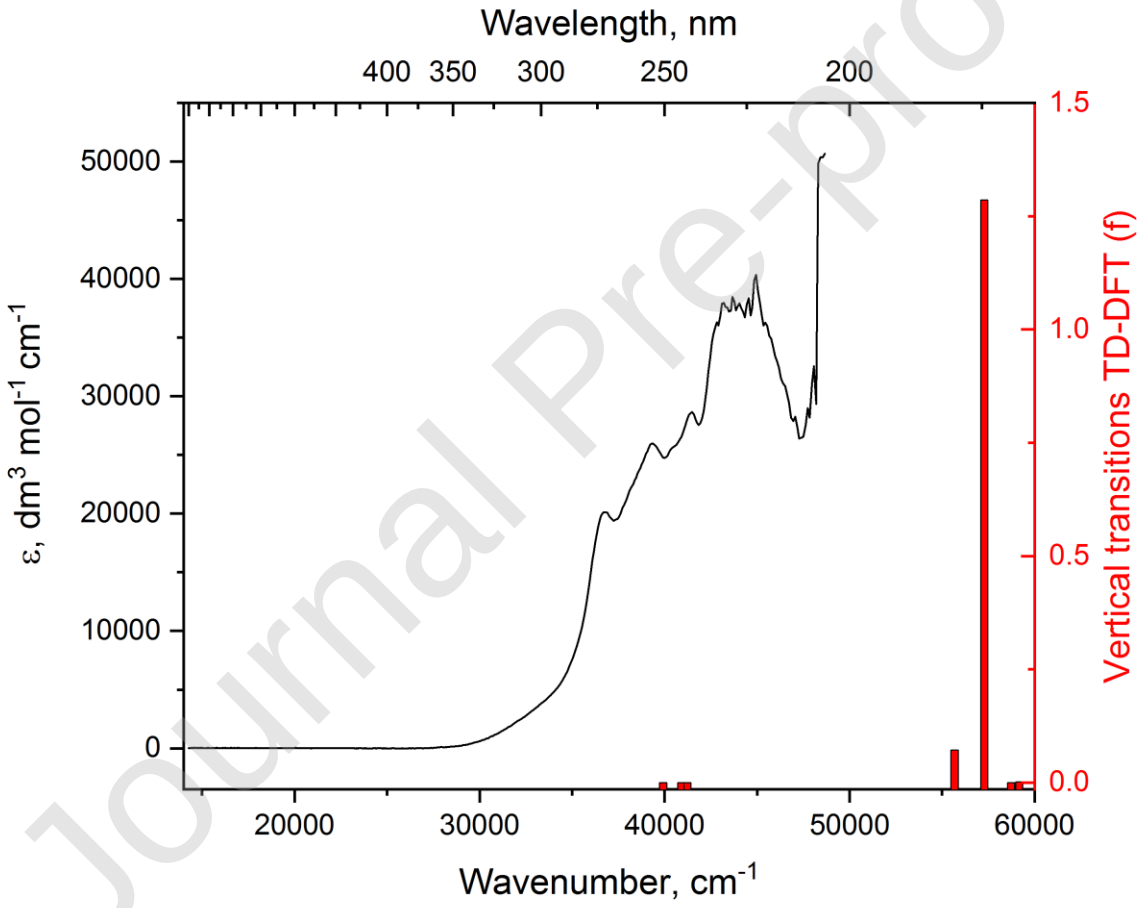

Figure 1. UV-Vis absorption spectrum of IC_3N, as measured for a gas-phase sample. Bars indicate the predicted location and oscillator strength of vertical electronic transitions, derived with TD-CAM-B3LYP/aug-cc-pVQZ.

Journal Pre-proof

IR spectroscopy

An IR absorption spectrum of IC_3N in Ar obtained for a sample deposited without photolysis (see Fig. 2) served as a reference for comparison with a photo-processed matrix. Fundamental vibrational bands have been identified based on data published (Table 2).[6,60] A high S/N ratio allowed assignment of new combination bands and of several spectral features belonging to ^{13}C and ^{15}N isotopologues of IC_3N present at their natural abundance (see Tables S2-S3 and the insets of Fig. 2); this was assisted with DFT predictions of isotopic shifts. Furthermore, it was possible to identify, for the first time, various combination and overtone vibrational bands of the molecule (Table 2). Several weak, unassigned bands may either be due to more complicated combinations of IC_3N vibrational modes or to impurities.

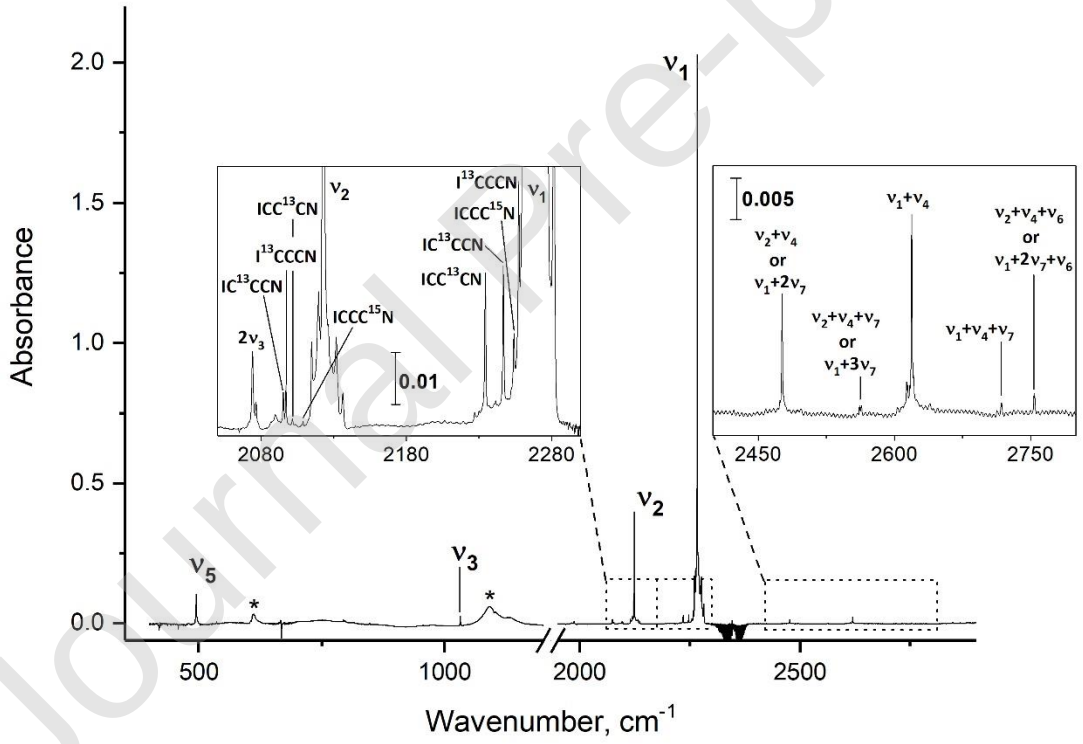

Figure 2. IR absorption spectrum of IC_3N in solid Ar at 15 K. Asterisked bands arise from incomplete compensation of CsI substrate absorption.

Journal Pre-proof

Theoretically considered IC_3N photolysis products

IC_3N is a halogenated analogue of the extensively studied molecule HC_3N. UV irradiation of the latter in inert cryogenic matrixes leads to HCCNC, HCNCC, and CCCNH.[1,62–64] We computed the electronic energies, structures, and vibrational IR absorption parameters of the 3 analogous isomers bearing iodine in place of hydrogen (Fig. 3). The ensuing relative energy values and molecular geometries turn out to be similar to those characterizing the HC_3N family of isomers. The most stable is the nitrile IC_3N, the isonitrile IC_2NC being more energetic by about 137 kJ/mol. Much less stable are two other chain structures: C_3NI and C_2NCI. No bound Y-shaped carbene structure $C_2(I)CN$, analogous to the cyanovinylidene molecule,[65–67] has been found in our B3LYP study, but CAM-B3LYP computations suggest the presence of a corresponding shallow potential energy minimum. IR spectroscopic parameters predicted for the lowest-energy IC_3N molecules can be found further in the text and in the Tables S3 – S5 of the Supplementary material.

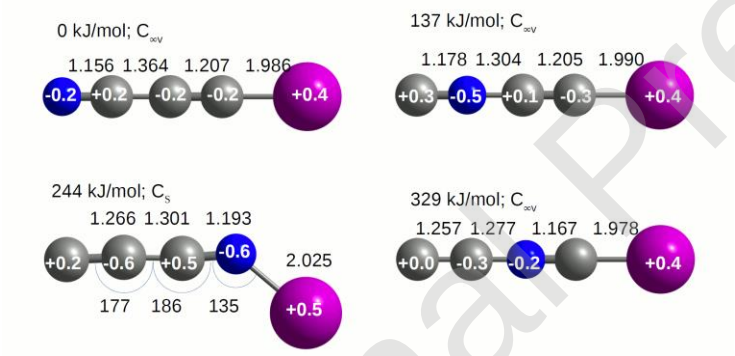

Figure 3. Relative ZPE-corrected electronic energies and structures (Å, deg) of the selected IC_3N isomers (NBO charges are given for each atom), as derived with B3LYP/aug-cc-pVTZ (aug-cc-pVTZ-PP for I atom). See Table S5 for the computed ionization energy and electron affinity values.

Table S5 of the Supplementary material presents ionization energies predicted for the four considered isomeric variants of IC_3N. What follows from these results is that none of the respective cations should be expected to appear out of IC_3N irradiated with the presently applied far-UV lamp ($\lambda > 127$ nm). Neither was any obvious source of electrons, leading to the corresponding anions, available in our experiment. Nevertheless, Table S5 provides also the

Journal Pre-proof

electron affinities, as these, together with the structural parameters given in Fig. S3, might be useful in the interpretation of future experiments. The calculated ionization energy of IC_3N (989 kJ/mol) is a good match to the value found experimentally, i.e. 974.5 kJ/mol (10.1 eV or 123 nm).[9]

Our theoretical treatment of permanent dissociation processes was limited here to the consideration of net thermodynamic effects confined to the ground-state potential energy surface. Reaction endothermicities were compared to the amount of supplied energy (equivalent to $\lambda >$ 127 nm). What follows is that one cannot rule out the dissociation of IC_3N into either $I+C_3N$, $ICN+C_2$ or IC_2+CN, while the heterolytic formation of ionic pairs, *e.g.* $I^+ + C_3N^-$, is not likely (Table S6). This simplistic approach does not allow us to conclude on the actual feasibility of the said homolytic cleavages, as it neglects the involvement of excited electronic states, possible energy barriers, and, of importance in cryogenic matrices, the *cage effect*.[68] The latter often curbs any durable separation of photofragments, giving preference to the stoichiometry-preserving molecular rearrangements.

Additionally, the possible formation of noble gas compounds $IArC_3N$ and IC_2ArCN has been computationally examined. The respective theoretical predictions are provided in Fig. S4 and Table S7 of Supplementary materials (present experiments gave no supportive evidence for these species).

Photolysis results and discussion

Far-UV photolysis of Ar matrix-isolated IC_3N led to the appearance of new bands in the IR absorption spectrum (see Fig. 4). The evolution of these was monitored over the course of the experiment. Thermal cycling (annealing) steps, involving the sample warm-up to approx. 22 K for about 6 minutes, followed by re-cooling to 15 K, was performed after the irradiation.

Journal Pre-proof

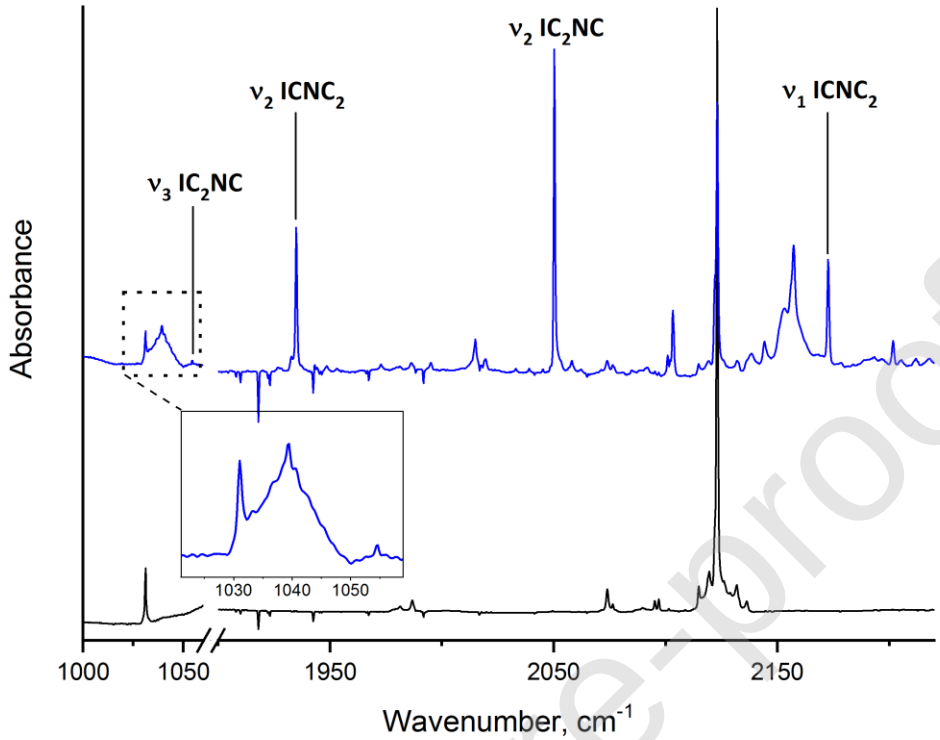

Figure 4. Bands of isomers in the IR absorption spectrum of VUV-photolyzed (λ > 127 nm) IC_3N isolated in solid Ar (upper trace). Bottom trace shows the spectrum of a non-irradiated sample. Absorbance scales are arbitrary.

In the case of IC_3N, the observed IR band intensity pattern was correctly reproduced by our DFT calculations (see Table 2). We assume a similar reliability of this theoretical approach applied to other closed-shell IC_3N-stoichiometry species.

Data gathered in Table 3 concern the identification of IC_2NC. A prominent IR absorption feature at 2050.2 cm^{-1} can be identified as ν_2. It is predicted for this isomer as the strongest one. The second strongest band, the one due to ν_6 bending, is expected at around 270 cm^{-1}, well beyond our available spectral range. The ν_3 stretching is predicted as 2 orders of magnitude less intense in IR than ν_2. Band strength data, collected throughout the photolysis, were helpful in the search for this weak feature. Correlations of integrated intensities, involving the postulated ν_2 band and

Journal Pre-proof

the ν_3 candidate bands at 1054.5 cm^{-1} (Fig. 5a) and 1039.5 cm^{-1} (Fig. 5b) were analyzed. Considering the extent of error bars, Fig. 5a shows (unlike Fig. 5b) quite a probable linear correlation. Common origin of the spectral features located at 2050.2 cm^{-1} and 1054.5 cm^{-1} is additionally suggested by their similar resistance to annealing (in contrast to the 1039.5 cm^{-1} band, slightly decreasing upon thermal treatment). Noteworthy, a broad hump centered at 1040 cm^{-1} is much too strong to be due to the ν_3 mode; its integrated intensity is almost the same as for the 2050.2 cm^{-1} band. In view of the above considerations, the sharp 1054.5 cm^{-1} feature is interpreted here as the ν_3 band of IC_2NC.

Journal Pre-proof

Journal Pre-proof

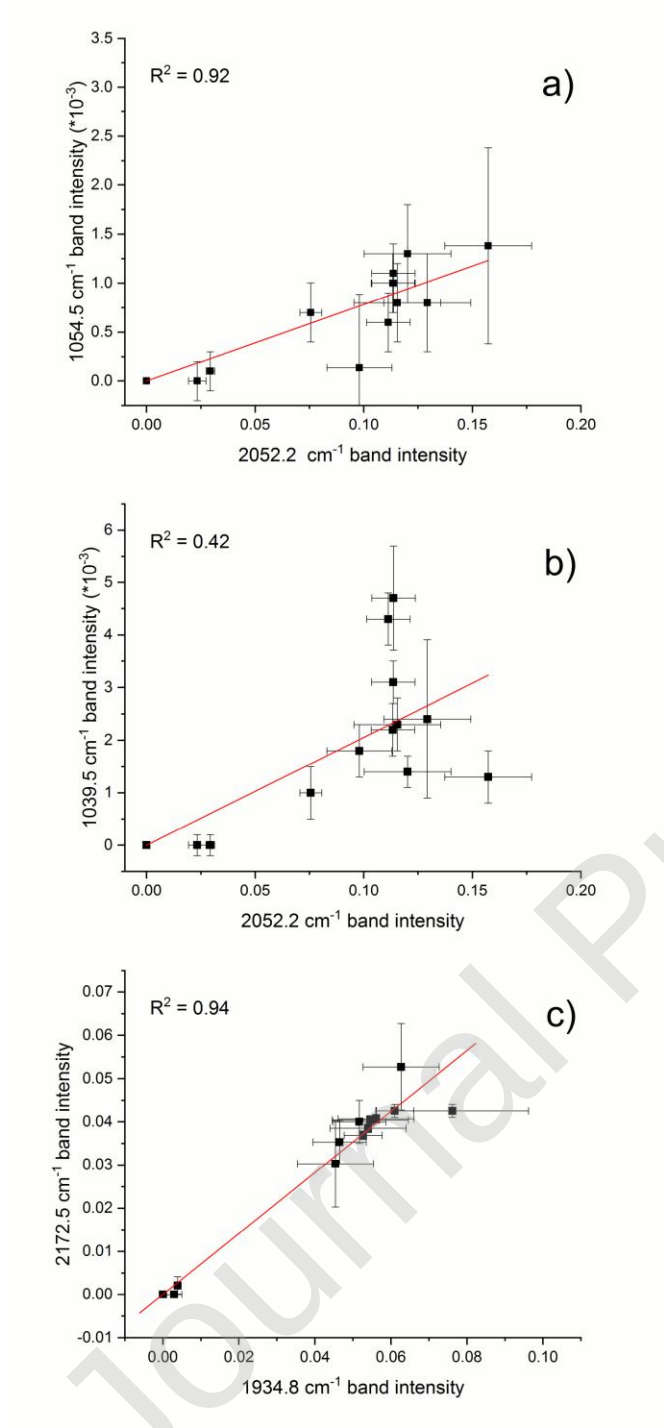

Figure 5. Correlation of the measured integrated optical density values for selected pairs of IR bands relevant to the identification of IC_2NC (*a, b*) and $ICNC_2$ (c), arising in the course of far-UV photolysis of IC_3N isolated in solid argon. Red lines represent least-squares linear fits.

Journal Pre-proof

Journal Pre-proof

The predicted frequency of the ν_5 bending vibration of IC_2NC formally falls within the spectral range of the instrument used, although a S/N decrease near 400 cm^{-1} prevented detection of the respective absorption. On the other hand, the IR spectrum is crowded with absorption features around the predicted IC_2NC ν_1 frequency. The anticipated separation of ν_1 and ν_2 is about 200 cm^{-1} at DFT and 220 cm^{-1} at CCSD(T) levels of theory. One can therefore expect to find the ν_1 band of IC_2NC at around 2260 ± 20 cm^{-1}. Theory describes it as even weaker than ν_3, and comparable in intensity to the bands of ^{13}C-isotopomers of the parent species, located in the same region (cf. Fig. 2). Without further studies, involving isotopically labeled precursor species or the application of Raman spectroscopy (indeed, the expected Raman activity and IR absorption intensity patterns significantly differ one from the other; see Table 3), it is impossible to assign any specific band to the ν_1 mode of IC_2NC.

We have carried out a theoretical study on the $IC_3N \rightarrow IC_2NC$ reaction, starting from the ground-state rearrangement, analyzed within the IRC scheme. Energies of the lowest excited singlet and triplet states were derived assuming vertical excitations from discreet IRC-obtained ground-state structures along the reaction coordinate. The result is depicted in Fig. 6. The computed ground-state activation energy (including zero-point energy contributions) amounts to 267 kJ/mol, a value similar to that reported for the analogous isomerization of HC_3N (272 kJ/mol).[69] This is well below the energies of any excited electronic state of IC_3N. When the parent molecule absorbs a vacuum-UV photon from a Kr lamp, the reaction may proceed by overcoming the barrier in an excited singlet state, with a possible crossing to the lowest triplet-state surface.

Journal Pre-proof

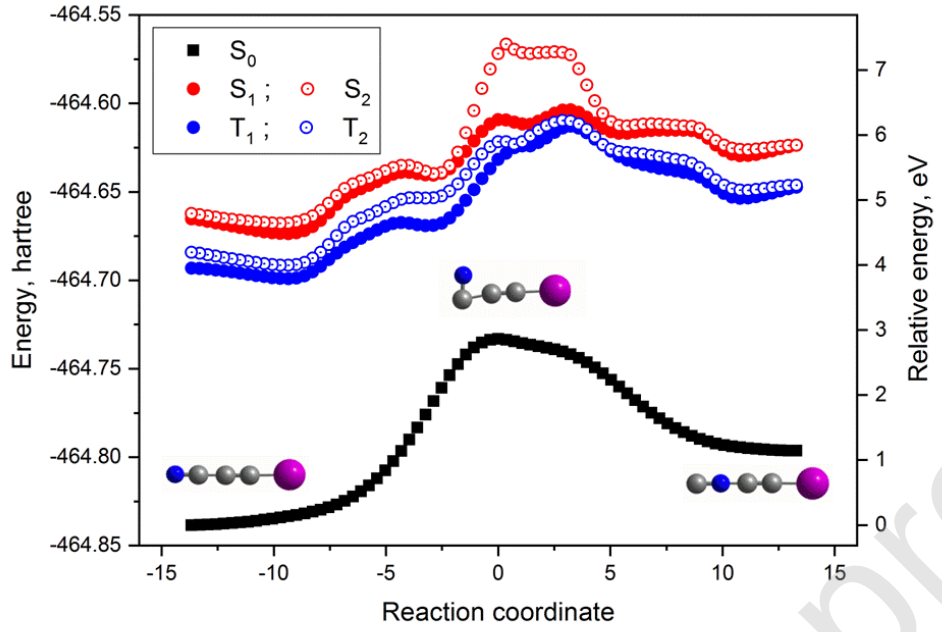

Figure 6. Ground- and selected excited-state cross-sections of IC_3N potential energy surfaces depicting the isomerization towards IC_2NC. The reaction coordinate comes from ground-state IRC calculations at the B3LYP/aug-cc-pVTZ (aug-cc-pVTZ-PP for I atom) level of theory. Molecular geometries corresponding to the two energy minima and a transition state are shown. Excited state energies were derived by TD-DFT calculations, departing from the respective ground-state geometries.

As demonstrated in Fig. 5c, spectral features observed at 2172.5 cm^{-1} and 1934.8 cm^{-1} are well correlated throughout the photolysis time. It was at first tempting to consider the C_3N^- anion as their possible common carrier. However, rather than a single 2172.5 cm^{-1} feature, the reported spectrum of C_3N^- coming from HC_3N photolysis in solid Ar revealed a Fermi-resonance doublet manifesting as two bands located at 2173.0 and 2178.0 cm^{-1}.[70,71] Secondly, a mismatch of about 10 cm^{-1} between 1934.8 cm^{-1} and the frequency of another HC_3N-derived anion band, 1944.0 cm^{-1}, is large, even considering some differences in local microenvironments (matrix cages) inherent to IC_3N and HC_3N experiments. Finally, the intensity ratio of 2172.5 cm^{-1} and 1934.8 cm^{-1} bands differs greatly from that reported for the two strongest C_3N^- IR absorption features produced upon the photolysis of HC_3N. The currently observed ratio matches decently, however, what is predicted for the $ICNC_2$ isomer, as do the frequencies of the two bands (see Table 4). In

Journal Pre-proof

view of the above, and considering that a similar rearrangement, $HC_3N \rightarrow HCNC_2$, has been observed for cyanoacetylene, we assign the said bands to $ICNC_2$.

According to our computations, UV photons available in this experiment are energetic enough (their spectrum extending from 9.76 eV to near-IR) to overcome all energy barriers separating IC_3N from $ICNC_2$. The initial step most likely involves $IC_3N \rightarrow IC_2NC$ isomerization, described above (Fig. 6). The path then proceeds (Fig. 7a) via a cyclic isomer. The latter species appears with a large excess of energy, which likely facilitates an efficient conversion towards $ICNC_2$ (Fig. 7b). While the exact identity of the involved potential energy surfaces is not known, the path may lead either through singlet or triplet states of the participating molecules.

Journal Pre-proof

Journal Pre-proof

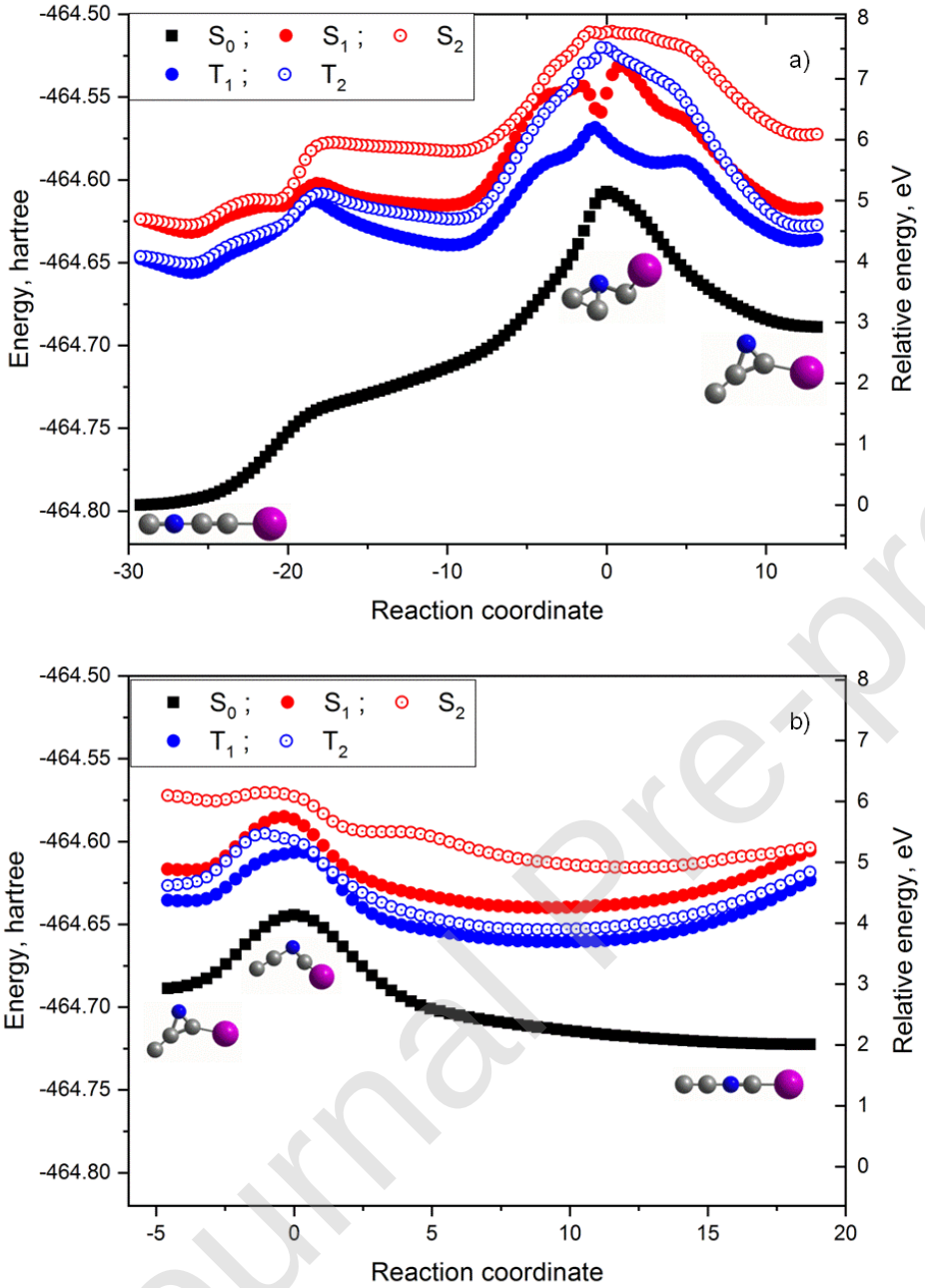

Figure 7. Ground- and selected excited-state cross-sections of IC_3N potential energy surfaces depicting a 2-step (panels *a* and *b*) isomerization path from IC_2NC to $ICNC_2$. The reaction coordinate comes from ground-state IRC calculations at the B3LYP/aug-cc-pVTZ (aug-cc-pVTZ-PP for I atom) level of theory. Molecular geometries corresponding to the energy minima and transition states are shown. Excited state energies were derived by TD-DFT calculations departing from the respective ground-state geometries.

Journal Pre-proof

Conclusions

There is experimental evidence, backed with theoretical predictions, for the formation of chain species IC_2NC and $ICNC_2$ upon far-UV photolysis of iodocyanoacetylene isolated in solid argon. The two isomeric species have not, to our knowledge, been observed before. IR-spectroscopic description of the parent IC_3N molecule has been appended with the assignment of additional combination bands. Several fundamental IR transitions of ^{13}C- and ^{15}N-isotopologues of IC_3N, present in their natural abundances, were identified. No IC_3N-related ions, in particular no C_3N^-, have been detected in the course of these experiments.

Declaration of interests

☐ The authors declare that they have no known competing financial interests or personal relationships that could have appeared to influence the work reported in this paper.

Acknowledgments

J.-C.G. thanks the Program PCMI (INSU-CNRS) and the Centre National d'Etudes Spatiales (CNES) for funding. Authors wish to thank Thomas Custer for valuable suggestions and comments on the manuscript.

Journal Pre-proof

Journal Pre-proof

References

(1) Kołos, R.; Waluk, J. Matrix-Isolated Products of Cyanoacetylene Dissociation. *J. Mol. Struct.* **1997**, *408–409*, 473–476. https://doi.org/10.1016/S0022-2860(96)09573-7.

(2) Coupeaud, A.; Kołos, R.; Couturier-Tamburelli, I.; Aycard, J. P.; Piétri, N. Photochemical Synthesis of the Cyanodiacetylene HC_5N: A Cryogenic Matrix Experiment. *J. Phys. Chem. A* **2006**, *110* (7), 2371–2377. https://doi.org/10.1021/jp055582r.

(3) Coupeaud, A.; Turowski, M.; Gronowski, M.; Piétri, N.; Couturier-Tamburelli, I.; Kołos, R.; Aycard, J.-P. Spectroscopy of Cyanodiacetylene in Solid Argon and the Photochemical Generation of Isocyanodiacetylene. *J. Chem. Phys.* **2007**, *126* (16), 164301. https://doi.org/10.1063/1.2720842.

(4) Kloster-Jensen, E.; Dyrssen, D.; Johansson, L.; Norén, B.; Munch-Petersen, J. Unsaturated Hydrogen-Free Halogeno Cyano Compounds. I. Synthesis and Properties of Iodocyanoacetylene. *Acta Chem. Scand.* **1963**, *17*, 1859–1861. https://doi.org/10.3891/acta.chem.scand.17-1859.

(5) Klaboe, P.; Kloster-Jensen, E. Raman Spectra and Revised Vibrational Assignments of Some Halogeno Cyanoacetylenes. *Spectrochim. Acta Part Mol. Spectrosc.* **1967**, *23*, 1981–1990. https://doi.org/10.1016/0584-8539(67)80085-0.

(6) Nolin, C.; Weber, J.; Savoie, R. Vibrational Spectra of Crystalline HCCN, DCCCN, ClCCCN, BrCCCN, and ICCCN. *J. Raman Spectrosc.* **1976**, *5* (1), 21–33. https://doi.org/10.1002/jrs.1250050104.

(7) Borgen, B.; Hassel, O.; Römming, Chr.; Block-Bolten, A.; Toguri, J. M.; Flood, H. Mutual Arrangement of Iodo-Cyano-Acetylene Molecules in the Solid. *Acta Chem. Scand.* **1962**, *16*, 2469–2470. https://doi.org/10.3891/acta.chem.scand.16-2469.

(8) Bieri, G.; Heilbronner, E.; Hornung, V.; Kloster-Jensen, E.; Maier, J. P.; Thommen, F.; Niessen, W. von. Electronic States of Substituted Haloacetylene and Cyanoacetylene Radical Cations. *Chem. Phys.* **1979**, *36*, 1–14. https://doi.org/10.1016/0301-0104(79)85099-5.

(9) Kuhn, R.; Maier, J. P.; Thommen, F. Photoelectron-Photon Coincidence Studies of the $\widetilde{A}$ and $\widetilde{B}$ excited Electronic States of X-C≡C-C≡N^+, X = CH_3, CD_3, Cl, Br, I. *J. Electron Spectrosc. Relat. Phenom.* **1984**, *34* (3), 253–260. https://doi.org/10.1016/0368-2048(84)80069-9.

Journal Pre-proof

(10) Becke, A. D. Density-functional Thermochemistry. IV. A New Dynamical Correlation Functional and Implications for Exact-exchange Mixing. *J. Chem. Phys.* **1996**, *104* (3), 1040–1046. https://doi.org/10.1063/1.470829.

(11) Lee, C.; Yang, W.; Parr, R. G. Development of the Colle-Salvetti Correlation-Energy Formula into a Functional of the Electron Density. *Phys. Rev. B* **1988**, *37* (2), 785–789. https://doi.org/10.1103/PhysRevB.37.785.

(12) Kendall, R. A.; Dunning Jr, T. H.; Harrison, R. J. Electron Affinities of the First-row Atoms Revisited. Systematic Basis Sets and Wave Functions. *J. Chem. Phys.* **1992**, *96* (9), 6796–6806. https://doi.org/10.1063/1.462569.

(13) Peterson, K. A.; Shepler, B. C.; Figgen, D.; Stoll, H. On the Spectroscopic and Thermochemical Properties of ClO, BrO, IO, and Their Anions. *J. Phys. Chem. A* **2006**, *110* (51), 13877–13883. https://doi.org/10.1021/jp065887l.

(14) Andersson, M. P.; Uvdal, P. New Scale Factors for Harmonic Vibrational Frequencies Using the B3LYP Density Functional Method with the Triple-ζ Basis Set 6-311+G(d,p). *J. Phys. Chem. A* **2005**, *109* (12), 2937–2941. https://doi.org/10.1021/jp045733a.

(15) Merrick, J. P.; Moran, D.; Radom, L. An Evaluation of Harmonic Vibrational Frequency Scale Factors. *J. Phys. Chem. A* **2007**, *111* (45), 11683–11700. https://doi.org/10.1021/jp073974n.

(16) Li, X.; Frisch, M. J. Energy-Represented Direct Inversion in the Iterative Subspace within a Hybrid Geometry Optimization Method. *J. Chem. Theory Comput.* **2006**, *2* (3), 835–839. https://doi.org/10.1021/ct050275a.

(17) Fukui, K. The Path of Chemical Reactions - the IRC Approach. *Acc. Chem. Res.* **1981**, *14* (12), 363–368. https://doi.org/10.1021/ar00072a001.

(18) Bauernschmitt, R.; Ahlrichs, R. Treatment of Electronic Excitations within the Adiabatic Approximation of Time Dependent Density Functional Theory. *Chem. Phys. Lett.* **1996**, *256* (4), 454–464. https://doi.org/10.1016/0009-2614(96)00440-X.

(19) Casida, M. E.; Jamorski, C.; Casida, K. C.; Salahub, D. R. Molecular Excitation Energies to High-Lying Bound States from Time-Dependent Density-Functional Response Theory: Characterization and Correction of the Time-Dependent Local Density Approximation Ionization Threshold. *J. Chem. Phys.* **1998**, *108* (11), 4439–4449. https://doi.org/10.1063/1.475855.

Journal Pre-proof

(20) Stratmann, R. E.; Scuseria, G. E.; Frisch, M. J. An Efficient Implementation of Time-Dependent Density-Functional Theory for the Calculation of Excitation Energies of Large Molecules. *J. Chem. Phys.* **1998**, *109* (19), 8218–8224. https://doi.org/10.1063/1.477483.

(21) Chantzis, A.; Laurent, A. D.; Adamo, C.; Jacquemin, D. Is the Tamm-Dancoff Approximation Reliable for the Calculation of Absorption and Fluorescence Band Shapes? *J. Chem. Theory Comput.* **2013**, *9* (10), 4517–4525. https://doi.org/10.1021/ct400597f.

(22) Wang, Y.-L.; Wu, G.-S. Improving the TDDFT Calculation of Low-Lying Excited States for Polycyclic Aromatic Hydrocarbons Using the Tamm–Dancoff Approximation. *Int. J. Quantum Chem.* **2008**, *108* (3), 430–439. https://doi.org/10.1002/qua.21510.

(23) Richard, R. M.; Herbert, J. M. Time-Dependent Density-Functional Description of the 1La State in Polycyclic Aromatic Hydrocarbons: Charge-Transfer Character in Disguise? *J. Chem. Theory Comput.* **2011**, *7* (5), 1296–1306. https://doi.org/10.1021/ct100607w.

(24) Hsu, C.-P.; Hirata, S.; Head-Gordon, M. Excitation Energies from Time-Dependent Density Functional Theory for Linear Polyene Oligomers: Butadiene to Decapentaene. *J. Phys. Chem. A* **2001**, *105* (2), 451–458. https://doi.org/10.1021/jp0024367.

(25) Cordova, F.; Doriol, L. J.; Ipatov, A.; Casida, M. E.; Filippi, C.; Vela, A. Troubleshooting Time-Dependent Density-Functional Theory for Photochemical Applications: Oxirane. *J. Chem. Phys.* **2007**, *127* (16), 164111. https://doi.org/10.1063/1.2786997.

(26) Perdew, J. P.; Chevary, J. A.; Vosko, S. H.; Jackson, K. A.; Pederson, M. R.; Singh, D. J.; Fiolhais, C. Atoms, Molecules, Solids, and Surfaces: Applications of the Generalized Gradient Approximation for Exchange and Correlation. *Phys. Rev. B* **1992**, *46* (11), 6671–6687. https://doi.org/10.1103/PhysRevB.46.6671.

(27) Perdew, J. P.; Chevary, J. A.; Vosko, S. H.; Jackson, K. A.; Pederson, M. R.; Singh, D. J.; Fiolhais, C. Erratum: Atoms, Molecules, Solids, and Surfaces: Applications of the Generalized Gradient Approximation for Exchange and Correlation. *Phys. Rev. B* **1993**, *48* (7), 4978–4978. https://doi.org/10.1103/PhysRevB.48.4978.2.

(28) Perdew, J. P.; Burke, K.; Wang, Y. Generalized Gradient Approximation for the Exchange-Correlation Hole of a Many-Electron System. *Phys. Rev. B* **1996**, *54* (23), 16533–16539. https://doi.org/10.1103/PhysRevB.54.16533.

(29) Szczepaniak, U.; Kołos, R.; Gronowski, M.; Chevalier, M.; Guillemin, J.-C.; Turowski, M.; Custer, T.; Crépin, C. Cryogenic Photochemical Synthesis and Electronic

Journal Pre-proof

Spectroscopy of Cyanotetracetylene. *J. Phys. Chem. A* **2017**, *121* (39), 7374–7384. https://doi.org/10.1021/acs.jpca.7b07849.

(30) Lamarre, N.; Gans, B.; Vieira Mendes, L. A.; Gronowski, M.; Guillemin, J.-C.; De Oliveira, N.; Douin, S.; Chevalier, M.; Crépin, C.; Kołos, R.; et al. Excited Electronic Structure of Methylcyanoacetylene Probed by VUV Fourier-Transform Absorption Spectroscopy. *J. Quant. Spectrosc. Radiat. Transf.* **2016**, *182* (Supplement C), 286–295. https://doi.org/10.1016/j.jqsrt.2016.06.020.

(31) Turowski, M.; Szczepaniak, U.; Custer, T.; Gronowski, M.; Kołos, R. Electronic Spectroscopy of Methylcyanodiacetylene (CH_3C_5N). *ChemPhysChem* **2016**, *17* (24), 4068–4078. https://doi.org/10.1002/cphc.201600949.

(32) Yanai, T.; Tew, D. P.; Handy, N. C. A New Hybrid Exchange–Correlation Functional Using the Coulomb-Attenuating Method (CAM-B3LYP). *Chem. Phys. Lett.* **2004**, *393* (1–3), 51–57. https://doi.org/10.1016/j.cplett.2004.06.011.

(33) Peterson, K. A.; Figgen, D.; Goll, E.; Stoll, H.; Dolg, M. Systematically Convergent Basis Sets with Relativistic Pseudopotentials. II. Small-Core Pseudopotentials and Correlation Consistent Basis Sets for the Post-d Group 16–18 Elements. *J. Chem. Phys.* **2003**, *119* (21), 11113–11123. https://doi.org/10.1063/1.1622924.

(34) Barone, V. Vibrational Zero-Point Energies and Thermodynamic Functions beyond the Harmonic Approximation. *J. Chem. Phys.* **2004**, *120* (7), 3059–3065. https://doi.org/10.1063/1.1637580.

(35) Barone, V. Anharmonic Vibrational Properties by a Fully Automated Second-Order Perturbative Approach. *J. Chem. Phys.* **2005**, *122* (1), 014108. https://doi.org/10.1063/1.1824881.

(36) Bloino, J.; Barone, V. A Second-Order Perturbation Theory Route to Vibrational Averages and Transition Properties of Molecules: General Formulation and Application to Infrared and Vibrational Circular Dichroism Spectroscopies. *J. Chem. Phys.* **2012**, *136* (12), 124108. https://doi.org/10.1063/1.3695210.

(37) Frisch, M. J.; Trucks, G. W.; Schlegel, H. B.; Scuseria, G. E.; Robb, M. A.; Cheeseman, J. R.; Scalmani, G.; Barone, V.; Mennucci, B.; Petersson, G. A. *Gaussian 09*; Gaussian, Inc., Wallingford CT, 2009.

Journal Pre-proof

(38) Christiansen, O. Vibrational Structure Theory: New Vibrational Wave Function Methods for Calculation of Anharmonic Vibrational Energies and Vibrational Contributions to Molecular Properties. *Phys. Chem. Chem. Phys.* **2007**, *9* (23), 2942–2953. https://doi.org/10.1039/B618764A.

(39) Rauhut, G.; Hrenar, T. A Combined Variational and Perturbational Study on the Vibrational Spectrum of P_2F_4. *Chem. Phys.* **2008**, *346* (1), 160–166. https://doi.org/10.1016/j.chemphys.2008.01.039.

(40) Christiansen, O. Møller–Plesset Perturbation Theory for Vibrational Wave Functions. *J. Chem. Phys.* **2003**, *119* (12), 5773–5781. https://doi.org/10.1063/1.1601593.

(41) Hampel, C.; Peterson, K. A.; Werner, H.-J. A Comparison of the Efficiency and Accuracy of the Quadratic Configuration Interaction (QCISD), Coupled Cluster (CCSD), and Brueckner Coupled Cluster (BCCD) Methods. *Chem. Phys. Lett.* **1992**, *190* (1), 1–12. https://doi.org/10.1016/0009-2614(92)86093-W.

(42) Deegan, M. J. O.; Knowles, P. J. Perturbative Corrections to Account for Triple Excitations in Closed and Open Shell Coupled Cluster Theories. *Chem. Phys. Lett.* **1994**, *227* (3), 321–326. https://doi.org/10.1016/0009-2614(94)00815-9.

(43) Pople, J. A.; Head-Gordon, M.; Raghavachari, K. Quadratic Configuration Interaction. A General Technique for Determining Electron Correlation Energies. *J. Chem. Phys.* **1987**, *87* (10), 5968–5975. https://doi.org/10.1063/1.453520.

(44) Raghavachari, K.; Trucks, G. W.; Pople, J. A.; Head-Gordon, M. A Fifth-Order Perturbation Comparison of Electron Correlation Theories. *Chem. Phys. Lett.* **1989**, *157* (6), 479–483. https://doi.org/10.1016/S0009-2614(89)87395-6.

(45) Bartlett, R. J.; Watts, J. D.; Kucharski, S. A.; Noga, J. Non-Iterative Fifth-Order Triple and Quadruple Excitation Energy Corrections in Correlated Methods. *Chem. Phys. Lett.* **1990**, *165* (6), 513–522. https://doi.org/10.1016/0009-2614(90)87031-L.

(46) Stanton, J. F. Why CCSD(T) Works: A Different Perspective. *Chem. Phys. Lett.* **1997**, *281* (1), 130–134. https://doi.org/10.1016/S0009-2614(97)01144-5.

(47) Rauhut, G. Efficient Calculation of Potential Energy Surfaces for the Generation of Vibrational Wave Functions. *J. Chem. Phys.* **2004**, *121* (19), 9313–9322. https://doi.org/10.1063/1.1804174.

Journal Pre-proof

(48) Hrenar, T.; Werner, H.-J.; Rauhut, G. Accurate Calculation of Anharmonic Vibrational Frequencies of Medium Sized Molecules Using Local Coupled Cluster Methods. *J. Chem. Phys.* **2007**, *126* (13), 134108. https://doi.org/10.1063/1.2718951.

(49) Neff, M.; Rauhut, G. Erratum: "Toward Large Scale Vibrational Configuration Interaction Calculations" [J. Chem. Phys. 131, 124129 (2009)]. *J. Chem. Phys.* **2009**, *131* (22), 229901. https://doi.org/10.1063/1.3273188.

(50) Rauhut, G.; El Azhary, A.; Eckert, F.; Schumann, U.; Werner, H.-J. Impact of Local Approximations on MP2 Vibrational Frequencies. *Spectrochim. Acta. A. Mol. Biomol. Spectrosc.* **1999**, *55* (3), 647–658. https://doi.org/10.1016/S1386-1425(98)00268-6.

(51) Hrenar, T.; Rauhut, G.; Werner, H.-J. Impact of Local and Density Fitting Approximations on Harmonic Vibrational Frequencies. *J. Phys. Chem. A* **2006**, *110* (5), 2060–2064. https://doi.org/10.1021/jp055578f.

(52) Eckert, F.; Pulay, P.; Werner, H.-J. Ab Initio Geometry Optimization for Large Molecules. *J. Comput. Chem.* **1997**, *18* (12), 1473–1483. https://doi.org/10.1002/(SICI)1096-987X(199709)18:12<1473::AID-JCC5>3.0.CO;2-G.

(53) Werner, H.-J.; Knowles, P. J.; Knizia, G.; Manby, F. R.; Schütz, M. Molpro: A General-Purpose Quantum Chemistry Program Package. *Wiley Interdiscip. Rev. Comput. Mol. Sci.* **2012**, *2* (2), 242–253. https://doi.org/10.1002/wcms.82.

(54) Werner, H.-J.; Knowles, P. J.; Knizia, G.; Manby, F. R.; Schütz, M.; Celani, P.; Korona, T.; Lindh, R.; Mitrushenkov, A.; Rauhut, G.; et al. *MOLPRO, Version 2012.1, a Package of Ab Initio Programs, See Http://Www.Molpro.Net*.

(55) Chemcraft - Graphical program for visualization of quantum chemistry computations, www.chemcraftprog.com http://www.chemcraftprog.com/ (accessed Oct 28, 2017).

(56) Kloster-Jensen, E.; Dyrssen, D.; Johansson, L.; Norén, B.; Munch-Petersen, J. Unsaturated Hydrogen-Free Halogeno Cyano Compounds. II. Synthesis and General Properties of Bromocyanoacetylene. *Acta Chem. Scand.* **1963**, *17*, 1862–1865. https://doi.org/10.3891/acta.chem.scand.17-1862.

(57) Bruston, P.; Poncet, H.; Raulin, F.; Cossart-Magos, C.; Courtin, R. UV Spectroscopy of Titan's Atmosphere, Planetary Organic Chemistry, and Prebiological Synthesis. *Icarus* **1989**, *78* (1), 38–53. https://doi.org/10.1016/0019-1035(89)90068-7.

Journal Pre-proof

(58) Job, V. A.; King, G. W. The Electronic Spectrum of Cyanoacetylene: Part I. Analysis of the 2600-Å System. *J. Mol. Spectrosc.* **1966**, *19* (1), 155–177. https://doi.org/10.1016/0022-2852(66)90238-4.

(59) Job, V. A.; King, G. W. The Electronic Spectrum of Cyanoacetylene: Part II. Analysis of the 2300-Å System. *J. Mol. Spectrosc.* **1966**, *19* (1), 178–184. https://doi.org/10.1016/0022-2852(66)90239-6.

(60) NIST Office of Data and Informatics. NIST Chemistry WebBook https://webbook.nist.gov/chemistry/ (accessed Sep 27, 2019). https://doi.org/10.18434/T4D303.

(61) *NIST Computational Chemistry Comparison and Benchmark Database, NIST Standard Reference Database Number 101 Release 20, August 2019, Editor: Russell D. Johnson III Http://Cccbdb.Nist.Gov/.*

(62) Khriachtchev, L.; Lignell, A.; Tanskanen, H.; Lundell, J.; Kiljunen, H.; Räsänen, M. Insertion of Noble Gas Atoms into Cyanoacetylene: An Ab Initio and Matrix Isolation Study. *J. Phys. Chem. A* **2006**, *110* (42), 11876–11885. https://doi.org/10.1021/jp063731f.

(63) Guennoun, Z.; Couturier-Tamburelli, I.; Piétri, N.; Aycard, J. P. UV Photoisomerisation of Cyano and Dicyanoacetylene: The First Identification of CCNCH and CCCNCN Isomers – Matrix Isolation, Infrared and Ab Initio Study. *Chem. Phys. Lett.* **2003**, *368* (5–6), 574–583. https://doi.org/10.1016/S0009-2614(02)01898-5.

(64) Kołos, R.; Sobolewski, A. L. The Infrared Spectroscopy of HNCCC: Matrix Isolation and Density Functional Theory Study. *Chem. Phys. Lett.* **2001**, *344* (5–6), 625–630. https://doi.org/10.1016/S0009-2614(01)00793-X.

(65) Goldberg, N.; Schwarz, H. Experimental Evidence for the Existence of Cyanovinylidene :C:C(H)CN. Gas-Phase Characterization of a Possible Interstellar Molecule. *J. Phys. Chem.* **1994**, *98* (12), 3080–3082. https://doi.org/10.1021/j100063a005.

(66) Hu, C. H.; Schaefer, H. F. Cyanovinylidene: An Observable Unsaturated Carbene and a Possible Interstellar Molecule. *J. Phys. Chem.* **1993**, *97* (41), 10681–10686. https://doi.org/10.1021/j100143a026.

(67) Kołos, R.; Gronowski, M.; Dobrowolski, J. Cz. Prospects for the Detection of Interstellar Cyanovinylidene. *Astrophys. J.* **2009**, *701* (1), 488–492. https://doi.org/10.1088/0004-637X/701/1/488.

Journal Pre-proof

(68) Bally, T. Matrix Isolation. In *Reactive Intermediate Chemistry*; John Wiley & Sons, Ltd, 2005; pp 795–845. https://doi.org/10.1002/0471721492.ch17.

(69) Yang, X.; Maeda, S.; Ohno, K. Global Analysis of Reaction Pathways on the Potential Energy Surface of Cyanoacetylene by the Scaled Hypersphere Search Method. *Chem. Phys. Lett.* **2006**, *418* (1), 208–216. https://doi.org/10.1016/j.cplett.2005.10.132.

(70) Kołos, R.; Gronowski, M.; Botschwina, P. Matrix Isolation IR Spectroscopic and Ab Initio Studies of C_3N^- and Related Species. *J. Chem. Phys.* **2008**, *128* (15), 154305. https://doi.org/10.1063/1.2902289.

(71) Turowski, M.; Gronowski, M.; Boyé-Péronne, S.; Douin, S.; Monéron, L.; Crépin, C.; Kołos, R. The C_3N^- Anion: First Detection of Its Electronic Luminescence in Rare Gas Solids. *J. Chem. Phys.* **2008**, *128* (16), 164304. https://doi.org/10.1063/1.2904876.

Journal Pre-proof

Journal Pre-proof

Table 1. Vertical excitation energies and oscillator strengths for electronic transitions of IC_3N, as computed with CAM-B3LYP/aug-cc-pVQZ.

State[a]	**Vertical energy eV (nm)**	**f**
$A\ ^1\Sigma^-$	4.95 (251)	0
$B\ ^1\Delta$	5.07 (245)	0
$C\ ^1\Delta$	5.11 (243)	0
$D\ ^1\Pi$	6.90 (180)	0.07
$E\ ^1\Sigma^+$	7.10 (175)	1.3

[a] States designated as the linear ones, irrespective of their equilibrium geometries, to ease the comparison with other cyanoacetylene family molecules.

Journal Pre-proof

Journal Pre-proof

Table 2. Comparison of computed and experimental IR absorption data for IC_3N.

Mode, symmetry	B3LYP [a]					CCSD(T)[b]			Experimental frequency, cm^{-1}		Rel. int. Ar
	ν_{harm},[c] scaled, cm^{-1}	IR int. harm., km/mol (relative int.)	Raman activity[d]	ν_{aharm}, cm^{-1}	I_{harm}/km mol^{-1}	ν_{harm}, cm^{-1}	ν_{aharm}, cm^{-1} VSCF	ν_{aharm}, cm^{-1} VMP2	IC_3N, gas [e] (solid)[f]	IC_3N:Ar	
ν_1, σ	2262	174 (100)	1381	2321	161	2316	2276	2273	2270 (2262)	2266.4	100
ν_2, σ	2126	21 (12)	80	2185	15	2155	2118	2115	2131 (21130	2123.1	13
ν_3, σ	983	1 (0.6)	1084	994	0.19	1000	988	1009	1031 (1037)	1031.1	0.8
ν_4, σ	347	0	645	359	0.01	356	353	353	364 (349)	out of range	
ν_5, π	517	4 (2.3)	1.5	532	5	494	498	498	496 (483)	493.9+494.9	5.2
ν_6, π	309	24 (14)	341	327	15	303	308	304	309 (323,322sh)	out of range	
ν_7, π	108	0	271	114	1.0	110	124	116	(118,134)	out of range	
$\nu_2+\nu_4+\nu_6$ or $\nu_1+2\nu_7+\nu_6$	2781									2753.8	0.1
$\nu_1+\nu_4+\nu_7$	271									2717.9	0.

Journal Pre-proof

	7										05
$\nu_1+\nu_4$	2609			2680	0.0008					2619.0	0.7
$\nu_2+\nu_4+\nu_7$ or $\nu_1+3\nu_7$	2581 2586									2562.4	0.05
$\nu_2+\nu_4$ or $\nu_1+2\nu_7$	2473 2478			2543	0.0005					2476.1	0.5
$2\nu_3$	1968			2016	0.19				(2087)	2074.0	0.7
$2\nu_5$	1035			1063, 1084[g]	0.2; 0.12				(958, 959)	955.1	0.06
$\nu_4+\nu_5$	864			890	$2 \cdot 10^{-6}$					846.8	0.13

[a] Basis sets aug-cc-pVTZ for C and N atoms, aug-cc-pVTZ-I-PP for iodine.

[b] Non-augmented versions of the basis sets used in DFT calculations were applied.

[c] Harmonic frequencies scaled by 0.96 (see Table S4 in the Supplementary material for an extended list of calculated overtone and combination bands).

[d] Harmonic approximation.

[e] Ref. 60.

[f] Ref. 6, values from Raman spectra if IR data not available, sh – shoulder band.

[g] Ref. 61.

Journal Pre-proof

Journal Pre-proof

Table 3. Comparison of theoretically predicted and experimental IR absorption data for IC_2NC.

Mode, symmetry	B3LYP[a]					CCSD(T)[b]			Experiment IC_3N:Ar matrix	
	ν_{harm}, scaled cm^{-1} [c]	IR int. harm. (relative), km/mol	Raman act. (relative) [d]	ν_{aharm}, cm^{-1}	I_{harm} km/mol	ν_{harm} cm^{-1}	ν_{aharm}, cm^{-1} VSCF	ν_{aharm}, cm^{-1} VMP2	ν, cm^{-1}	Relative IR intensity
1, σ	2228	2 (1.1)	2054 (100)	2287	2 (1.2)	2295	2250	2253	not observed	
2, σ	2039	179 (100)	144 (7.0)	2090	168 (100)	2079	2036	2033	2050.2	100
3, σ	1038	6 (3.4)	1238 (60)	1078	3 (1.8)	1056	1042	1048	1054.5	1.3
4, σ	349	0 (0)	423 (21)	358	0.4 (0.2)	361	358	357	out of range	
5, π	442	2 (1.1)	64 (3.1)	449	0.12 (0.1)	422	426	424	not observed	
6, π	270	17 (9.5)	397 (19)	278	11 (6.5)	264	277	274	out of range	
7, π	112	0 (0)	324 (16)	116	0.3 (.2)	113	131	116	out of range	

[a] Basis set aug-cc-pVTZ with aug-cc-pVTZ-PP for I atom.

[b] Basis set cc-pVTZ with cc-pVTZ-PP for I atom.

[c] DFT frequencies scaled by 0.96 (see Table S8 in the Supplementary material for the predicted overtone and combination bands).

[d] Harmonic approximation.

Journal Pre-proof

Table 4. Comparison of the theoretically predicted and experimental IR absorption data for $ICNC_2$.

	Computations					Experiment	
Mode	**B3LYP[a]**				**CCSD(T)[b]**	**Ar matix**	
	ν_{harm},[c] cm^{-1}	I_{harm}, km mol^{-1} (rel. int.)	ν_{anharm}, cm^{-1}	I_{anharm}, km mol^{-1} (rel. int.)	ν_{harm}, cm^{-1}	Freq, cm^{-1}	I_{rel}
ν_1	2189	660 (100)	2231	590 (89)	2203	2172.5	71
ν_2	1950	630 (96)	1988	660 (100)	1966	1934.8	100
ν_3	1030	16 (2.4)	1074	14 (2.1)	1043	not observed	
ν_4	357	1.4 (0.2)	378	0.7 (0.1)	366	not observed	
ν_5	457	5.7 (0.9)	458	6.7 (1.0)	449	not observed	
ν_6	198	6.8 (1.0)	177	5.8 (0.9)	185	not observed	
ν_7	63	6.6 (1.0)	32	6.6 (1.0)	61	not observed	

[a] Basis set aug-cc-pVTZ with aug-cc-pVTZ-PP for I atom.

[b] Basis set cc-pVTZ with cc-pVTZ-PP for I atom.

[c] DFT frequencies scaled with 0.96 (see Table S9 in the Supplementary material for the list of calculated overtone and combination bands).

Journal Pre-proof